

First-principles calculations of the electronic structure and optical properties of LiB_3O_5 , CsB_3O_5 , and BaB_2O_4 crystals

Jun Li, Chun-gang Duan, Zong-quan Gu, and Ding-sheng Wang

Laboratory for Surface Physics, Institute of Physics, and Center for Condensed Matter Physics, Academia Sinica, Beijing 100080, China

(Received 2 September 1997)

This paper reports the calculation of electronic structure and linear optical properties of LiB_3O_5 (LBO), CsB_3O_5 (CBO), and BaB_2O_4 (BBO) crystals using the linearized augmented plane-wave band method. It is found that the top of their valence bands consists of O orbitals, while the boron has almost no contribution. The linkage between $(\text{B}_3\text{O}_7)^{5-}$ anionic groups in the crystalline state is the main cause of making the gap of LBO and CBO larger than BBO's. The near-edge interband transition contains the contribution of the trigonal coordinated B-O bands in the final state for LBO. For CBO and BBO, the final state consists mainly of cation states at the bottom of the conduction bands. In this case, however, the transition from the O derived valence states to these cation states is quite weak; strong transition only appears till about 1 eV above the absorption edge when B-O orbitals are also involved in the final states. [S0163-1829(98)02911-7]

I. INTRODUCTION

Borate crystals, such as lithium triborate LiB_3O_5 (LBO), cesium triborate CsB_3O_5 (CBO), and β -barium borate BaB_2O_4 (BBO), are developed as an important series of ultraviolet inorganic nonlinear optical (NLO) materials for second harmonic generation by Chen and his colleagues.¹⁻³ According to Chen's anionic group theory,⁴ the macroscopic NLO susceptibility of the crystals is the geometric superposition of the microscopic NLO susceptibility of all anionic groups in the crystals, which can be calculated from the localized wave functions of those anionic groups by a perturbation theory. From this theoretical analysis, characteristics of BBO have been elucidated, and further prediction has led to the discovery of LBO crystal.^{2,5}

Because of the obvious relation between the optical properties and their anionic groups, LBO and BBO have stirred up several theoretical interpretations. The controversy focuses on what role the cation plays in the optical properties of these borates or, in other words, to what extent the optical transition is influenced by the cations as, in particular, the heavy elements such as barium or cesium are involved. French *et al.*⁶ used the discrete variational multiple scattering cluster method to calculate the electronic structure of the anionic groups of LBO and BBO. They attributed the fundamental band-gap transition in both borates to the transitions between the states within the anionic groups, while the cation states are almost neglected. This type of cluster calculation is usually questionable as used for LBO where the anionic groups are closely connected. Xu and Ching,⁷ and Xu, Ching, and French⁸ studied the electronic structures and linear optical properties of LBO and BBO using the first-principles orthogonalized linear combination of atomic orbitals band method. They conjectured that the anisotropies in the layered structure of the anionic groups in BBO might account for its large nonlinear optical coefficient, while the nonlinearity of LBO may originate from the difference of the two types of its B-O groups. Hsu and Kasowski⁹ used the pseudofunction energy band method to perform self-

consistent *ab initio* electronic structure calculations for BBO and LBO. They found that the gap edge transition in LBO is between the states within the anionic group; in contrast, for BBO, it results from the valence states of the anionic group to the conduction cation states. Thus they questioned the validity of the cluster approximation of the anion group to BBO. Cheng and Lu¹⁰ used the INDO/S method with configuration interactions to calculate the electronic states of $\text{Li}_2\text{B}_6\text{O}_{10}$ and $\text{Ba}_3(\text{B}_3\text{O}_6)_2$ clusters. They found also that the barium cation has significant contribution to the band edge optical transition and the second order susceptibility in BBO, in contrast to the lithium of the LBO.

It is worth noting the difference and similarity between LBO, CBO and BBO crystals in the analysis of their optical properties. Both LBO and CBO are orthorhombic, with the space group $Pn2_1a$ (Ref. 11) and $P2_12_12_1$ (Ref. 12), respectively; and contain four formula units, i.e., 36 atoms, in one unit cell, with the $(\text{B}_3\text{O}_7)^{5-}$ anionic group [shown in Fig. 1(a)] as their structure unit. The average B-O bond lengths around the trigonal and tetrahedral coordinated boron atoms are 1.371 and 1.476 Å in LBO, respectively, and are 1.367 and 1.473 Å in CBO. This tiny difference in their anionic groups (less than 0.3%) implies that the change of their physical properties as well as the symmetry from LBO to CBO crystals should be attributed to the difference of their cations. On the other hand, BBO crystallizes in the trigonal crystal system with the space group $R3c$,¹³ and contains six formula units (42 atoms) per unit cell with the $(\text{B}_3\text{O}_6)^{3-}$ anionic group [shown in Fig. 1(b)] as its structure unit. The cations Cs^+ in CBO and Ba^{2+} in BBO belong to the same isoelectronic group of xenon, i.e., they have qualitatively similar electronic structure. It is expected that they exert a similar impact on the physical properties of materials containing them. Thus the comparison between CBO and BBO may shine lights on the difference of the effect of anionic groups $(\text{B}_3\text{O}_7)^{5-}$ and $(\text{B}_3\text{O}_6)^{3-}$. Unfortunately, in previous literatures there was no calculation on the CBO crystal to provide such information.

Besides these difference and similarity among the components of LBO, CBO, and BBO crystals, the geometry stacks of these components makes BBO distinct from LBO and

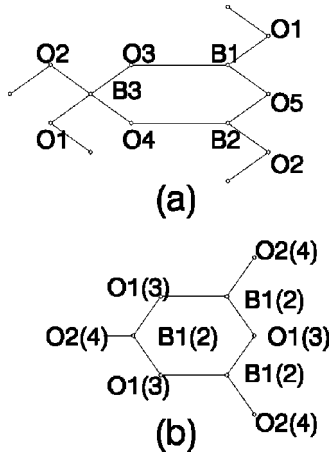


FIG. 1. Anionic groups (a) $(\text{B}_3\text{O}_7)^{5-}$ in the LBO and CBO crystals, which have all atoms nearly in one plane except that the two oxygen atoms (O1 and O2) near B3 deviate up and down from the plane, and all off-ring O1 and O2 atoms are linked to B atoms of neighboring anionic groups; (b) $(\text{B}_3\text{O}_6)^{3-}$ in the BBO crystal, which has all atoms nearly in one plane, and is nearly isolated from other anionic groups. The label for each atom represents the equivalency in the crystal environment. Because there are two inequivalent $(\text{B}_3\text{O}_6)^{3-}$ groups in one unit cell of BBO crystal, each atom has two labels.

CBO. Because of the bridging of the tetrahedral coordinated B, the $(\text{B}_3\text{O}_7)^{5-}$ anion groups have linked to each other to form an endless network in both LBO and CBO, with cations located in the interstices to grant the whole structure neutralization. In contrast, for the lack of such bridging in BBO, the $(\text{B}_3\text{O}_6)^{3-}$ anionic groups arrange in a layered planar structure with the Ba^{2+} making links between alternating $(\text{B}_3\text{O}_6)^{3-}$ layers. In other words, the interaction among $(\text{B}_3\text{O}_7)^{5-}$ groups is stronger than that among $(\text{B}_3\text{O}_6)^{3-}$ groups. The effect of this interaction among $(\text{B}_3\text{O}_7)^{5-}$ groups is also most likely neglected in a cluster calculation.

All these factors should affect the electronic structure of LBO, CBO, and BBO crystals in their own way, and consequently on their optical transition. A first-principles band calculation could reveal all these effects in a natural way. By appropriate analysis, these effects of (i) anionic groups $(\text{B}_3\text{O}_7)^{5-}$ or $(\text{B}_3\text{O}_6)^{3-}$, (ii) light cation Li^+ or heavy cations Cs^+ and Ba^{2+} , and (iii) linkage or isolation between clusters are expected to be recognized and understood. This is the very goal of the present paper. Because of the complexity of the borate crystals, the present study is confined to the electronic structure and linear optical transition, which

also gives strong hints on the understanding of the mechanism of the NLO transition.

The organization of this paper is straightforward. Section II discusses the electronic structure of LBO, CBO, and BBO crystals, based on our first-principles band calculation using the linearized augmented plane-wave (LAPW) method. This section consists of a comparison of LBO with CBO, a comparison of CBO with BBO, and also a comparison of our results with available experimental data and other band calculations. Section III treats the linear optical properties of these borate crystals: The methodology is sketched in this section while its validity to wide gap materials is discussed elsewhere already.¹⁴ The linear absorption spectra in the near edge region are discussed in detail, which reveals the mechanism of the optical transition between orbitals of different ions. Section IV presents an extended discussion and conclusion.

II. ELECTRONIC STRUCTURES

In this paper, the self-consistent LAPW method^{15,16} with the von Barth–Hedin exchange-correlation term is employed to carry out the band-structure calculation. The lattice parameters^{11–13} used in the calculation are listed in Table I. The muffin-tin radii of Li, Cs, Ba, B, and O are set equal to about 1.00, 1.60, 1.70, 0.50, and 0.83 Å, respectively. About 40 LAPW bases per atom are used in solving the semirelativistic Schrödinger equation, and 4, 8, and 4 special \vec{k} points in the irreducible Brillouin zone are used for LBO, CBO, and BBO crystals, respectively, in generating the charge density in the self-consistent calculation. The convergence measured by the rms difference between input and output charge density is better than $0.05me/(a.u.)^3$. Because of the requirement of large memory space in these calculations, a massively parallel processing computer with distributed memory (DAWN1000 made by Chinese National Research Center of Intelligent Computing) was used to carry out most part of the calculation. To deal with the large matrix diagonalization on distributed memory computers, a highly efficient parallel solver of the generalized eigenvalue problem^{17,18} is adopted.

The calculated band gap is listed in Table I. From our calculation, both LBO and CBO are direct gap crystals, while BBO are indirect gap crystal. However, for BBO the direct gap at Γ is only 0.03 eV larger than the indirect band gap from Γ to Z, which is in fact not larger than the possible error of present calculation. The trend of the band gap of three borates is in good agreement with the measured trend

TABLE I. Lattice constants, the angle (α) between any two crystal axes, and the energy gaps of LBO, CBO, and BBO crystals.

	a (Å)	b (Å)	c (Å)	α	Expt.	E_g (eV)		
						Present	Ref. 8	Ref. 9
LBO	8.46	5.13	7.38	90°	7.78 ^a	Γ : 6.95	Γ : 7.37	6.9
CBO	6.213	8.521	9.170	90°	7.28 ^b	Γ : 5.86		
BBO	8.380			96.65°	6.43 ^a	Γ -Z: 4.85 Γ : 4.88	Γ -X: 5.52 Γ : 5.6	4.9

^aReference 6.

^bReference 3.

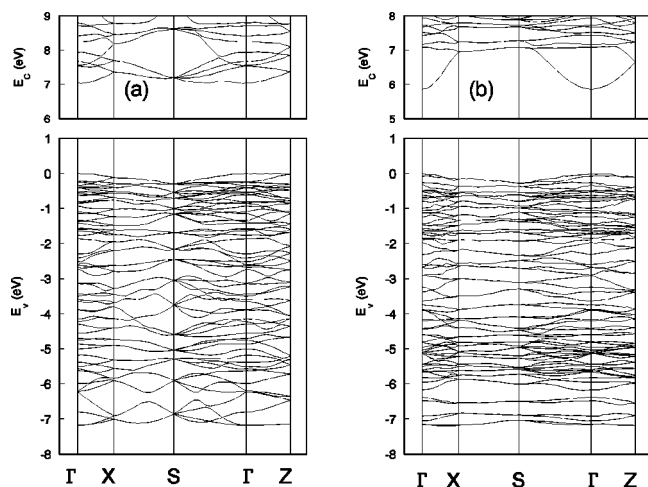


FIG. 2. Band structures of (a) LBO and (b) CBO crystals.

though their absolute values are all lower than the experimental data as expected in the framework of the local density approximation (LDA).

A. Comparison of LBO with CBO

The band structures of LBO and CBO crystals are plotted along symmetry lines in Figs. 2(a) and 2(b), respectively, in the energy scale for the convenience of the views. The energy reference is set to the top of the valence bands. Although LBO and CBO have different symmetry, their valence bands (VB's) are very flat and qualitatively similar to each other. The obvious difference occurs at the bottom of their conduction band (CB) that a band of large dispersion spanning about 1 eV appears in CBO crystal. Figure 3 is the total density of states (DOS) for LBO and CBO, which are calculated at 36 special \vec{k} points. The similarity in their VB region is clear: only a local band of Cs 5*p* semicore electrons [Fig. 4(b)] at -5 eV adds to the otherwise nearly identical O derived orbitals [Figs. 5(a) vs 5(b), and 5(c) vs 5(d)]. Figures 6(a) and 6(b) are the partial DOS projected on the trigonal B1 of LBO and CBO, respectively, and Figs. 6(c) and 6(d) on tetrahedral B3. These figures show that, in the very top of the VB (from 0 to -1 eV), there is no obviously hybridization between B and O atoms. The VB top is the mixture of the *p* states of O2 and O3. The highest occupied *p*-like states of boron atoms is about -0.34 eV in Figs. 6(a) and 6(c), and much lower in Figs. 6(b) and 6(d).

In the calculation of the isolated $(B_3O_7)^{5-}$ group,⁶ the highest occupied molecular orbital (HOMO) is a kind of dan-

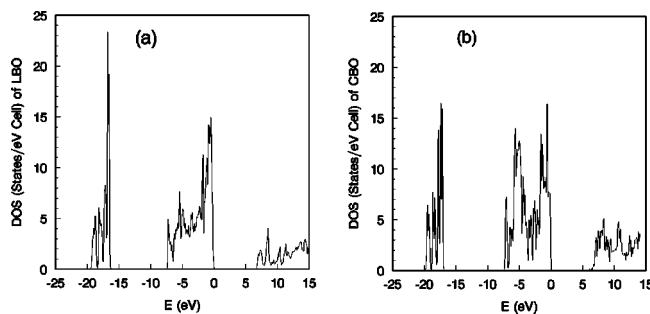


FIG. 3. Total DOS of (a) LBO and (b) CBO crystals.

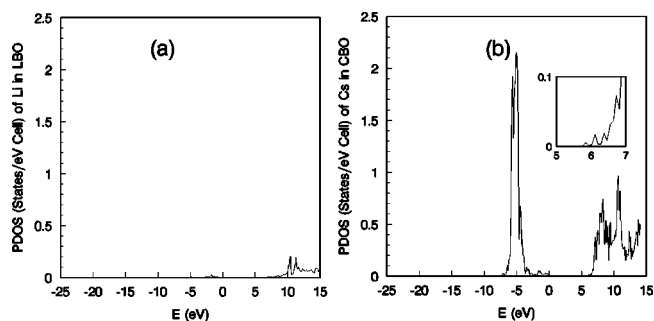


FIG. 4. Partial DOS projected on the cations (a) Li of LBO and (b) Cs of CBO crystals.

gling bonds arising from the off-ring O1 and O2, which is 2.54 eV higher than the nearest lower B-O bond orbitals. In the calculation of a larger $Li_2B_6O_{10}$ (Ref. 10) cluster, also cut from the LBO, where some off-ring O1 (or O2) have been linked with B atoms, the energy differences from HOMO to the nearest lower B-O bond is 0.84 eV. So from the isolated anionic group, through the larger cluster, to the crystal, the linkage between the anionic groups by the tetrahedral B atoms makes the dangling HOMO bonds evolve into the top of VB through interaction with the molecular orbitals at O3 (or O4). According to the energy difference between the HOMO dangling bonds and the nearest lower B-O bonds, it is estimated that the linkage of the anionic groups lowers the energy of the HOMO dangling bond, and enlarges the energy gap of the anionic group by about 2.2 eV (the difference between the previous cluster result, 2.54 eV, and the present band result, 0.34 eV). This effect relates only to the linkage of the anionic groups, but is independent of the type of cations. From this analysis, it is also doubtful to simply eliminate the HOMO dangling states for the estimation of the band gap as done in some anionic group calculations.⁶

It is interesting that for both LBO and CBO crystals the tetrahedral B3 gives no contribution in the neighborhood of

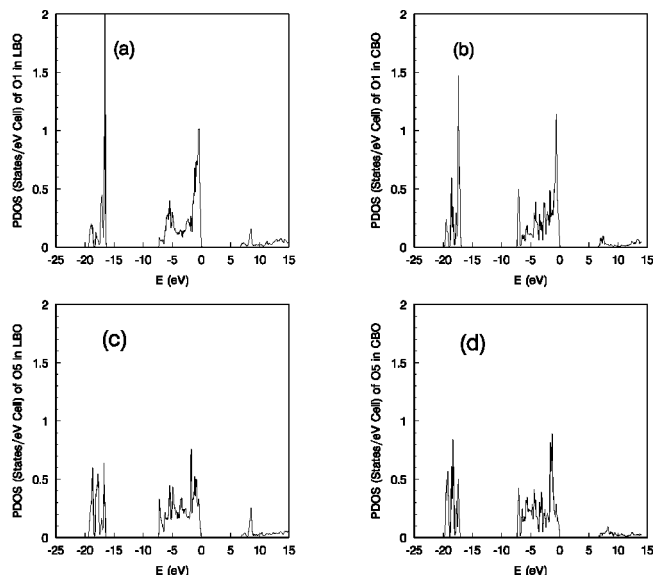


FIG. 5. Partial DOS projected on the oxygen atoms of LBO and CBO crystals. Those on O2, O3, and O4 atoms are similar to that on O1.

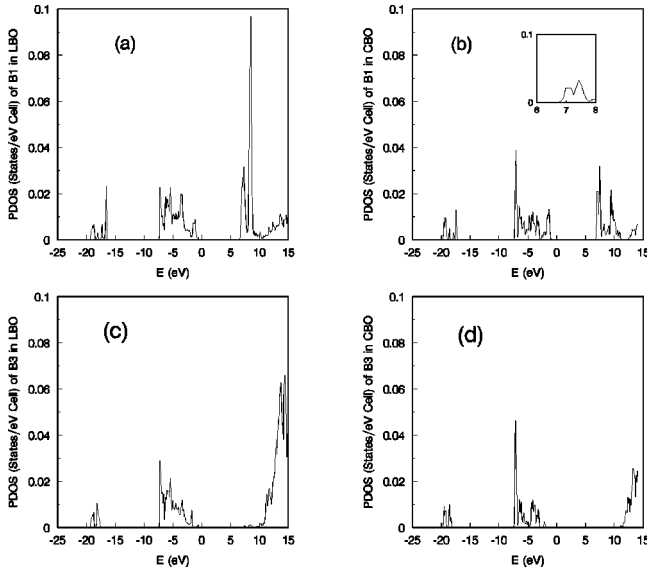


FIG. 6. Partial DOS projected on the boron atoms of LBO and CBO crystals. That on B2 is similar to that on B1.

the CB bottom, which implies that the states in the low-lying CB's are only in the plane of the B-O rings. The trigonal B1, however, enters CB right starting from its bottom. In contrast to LBO, it does not enter the bottom of CB in CBO [see the inset of Fig. 6(b)]. The cause is in fact that the Cs 6s state lies below the lowest unoccupied molecular orbital (LUMO) of the anionic group in the crystalline state. This can be seen more clearly in, and has profound effect on, the linear absorption spectra discussed below. While lithium has little contribution to the CB [Fig. 4(a)], cesium exerts obvious affection on the CB states [see Fig. 4(b)]. The three peaks in the CB DOS curves [Fig. 4(b)] are mainly the Cs 6s, 5d, and 4f states, respectively. Thus as the atomic number of the cation increases, the structure of CB states has been fundamentally changed.

The effect of the linkage between the anionic groups also manifests itself in the change of the core levels. The differ-

ence among the binding energies of 1s core electrons between the trigonal and tetrahedral coordinated boron atoms is less than 0.5 eV and between off-ring O1 (O2) and in-ring O3 (O4) atoms less than 0.4 eV in both LBO and CBO (see Table II). It is much smaller than that of the BBO (2.88 eV). This indicates that although those boron (oxygen) atoms are distinct from each other in the isolated $(B_3O_7)^{5-}$ groups, they become nearly equivalent in the crystalline environment for the bridging of the tetrahedral coordinated B. Only the in-ring O5, which makes a neighbor with only trigonal B atoms, is different from the off-ring O1 (O2). This in-ring O5 is different from the in-ring O3 (O4) atoms as seen also from their core levels (Table II). However, the $(B_3O_7)^{5-}$ anionic groups in LBO and CBO form different frameworks to embrace the different cations. The difference in the cation radii (Li^+ and Cs^+ are 0.60 and 1.69 Å,¹⁹ respectively) makes the unit cell of CBO 50% larger than LBO. Though the structure of their anionic groups remains unchanged, the expansion of the unit cell has the crystalline environments changed, and results in different binding energy shifts between the trigonal B and tetrahedral B, and between the off-ring and in-ring oxygen atoms.

B. Comparison of CBO with BBO

According to the isolated cluster calculation, the gap of $(B_3O_6)^{3-}$ from HOMO to LUMO is 6.2 eV,⁶ which is larger than that of $(B_3O_7)^{5-}$, 5.03 eV. However, according to the above analysis, the linkage of $(B_3O_7)^{5-}$ in crystalline states will enlarge the gap by 2.2 eV. From this point of view, the gap of CBO crystal consisting of linked $(B_3O_7)^{5-}$ groups should be about 1.0 eV larger than that of BBO consisting of rather isolated $(B_3O_6)^{3-}$ groups. It is indeed comparable to the measured gap difference of 0.85 eV (Table I).

Table II also shows that for CBO the difference of 1s core levels between the in-ring O3 (O4) and off-ring O is small, but in BBO the off-ring O2 (or O4) levels deviate from the in-ring O1 (or O3) by as large as 2.88 eV. Such a large chemical shift implies two distinguished oxygen environ-

TABLE II. Binding energies and level shift of 1s core electrons of boron and oxygen atoms in LBO, CBO, and BBO crystals (unit: eV, reference to the top of valence band).

	LBO	CBO	BBO
Trigonal B	Aver. -162.51	Aver. -155.46	Aver. -155.81
	B1 -162.64	B1 -155.57	B1 -155.75
	B2 -162.37	B2 -155.35	B2 -155.86
Tetrahedral B	B3 -162.04	B3 -155.39	
Tri. B-Tet. B	-0.47	-0.07	
Off-ring O	Aver. -496.80	Aver. -494.27	Aver. -493.53
	O1 -496.74	O1 -494.21	O2 -493.46
	O2 -496.86	O2 -494.32	O4 -493.60
In-ring O	Aver. -497.05	Aver. -494.69	Aver. -496.41
	O3 -496.98	O3 -494.84	O1 -496.22
	O4 -497.12	O4 -494.54	O3 -496.60
Off O-In O	0.25	0.42	2.88 (2.4 ^a)
In-ring O	O5 -497.41	O5 -495.30	
(O1, 2, 3, 4)-O5	0.48	0.81	

^aExperimental value evaluated from Fig. 6 in Ref. 6.

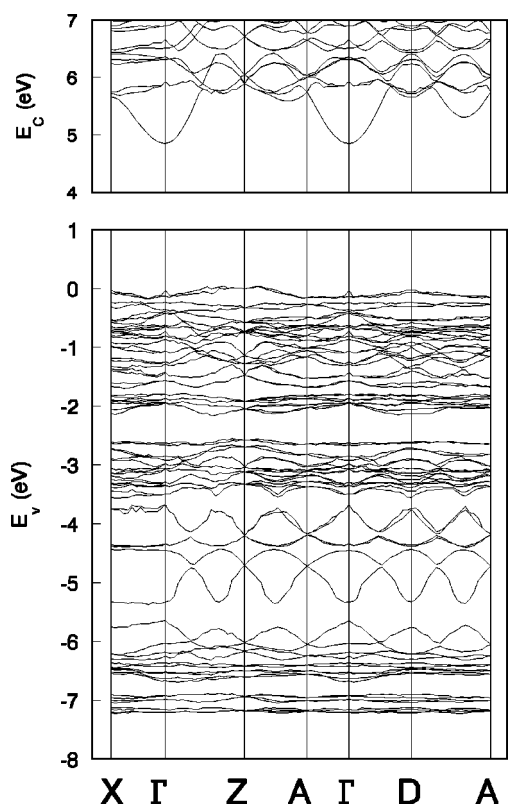


FIG. 7. Band structure of BBO crystal.

ments indicating that the $(B_3O_6)^{3-}$ groups keep the isolating features in BBO. The VB of BBO has a clear feature of the local molecular orbitals (Figs. 7, 8, and 9). The VB top also originates from the dangling bonds as of the isolated $(B_3O_6)^{3-}$ group. The antibonding σ bands, locating around -2 eV, arising from the in-ring oxygens. The π bonds of in-ring and off-ring oxygens form a wide band in the plot from -3 eV to -6 eV. Below -6 eV in Fig. 7 are the bands of the σ bonds of the in-ring oxygens. So clearly a local orbital feature is not seen in the band structure of CBO for the strong mixtures of the molecular orbitals.

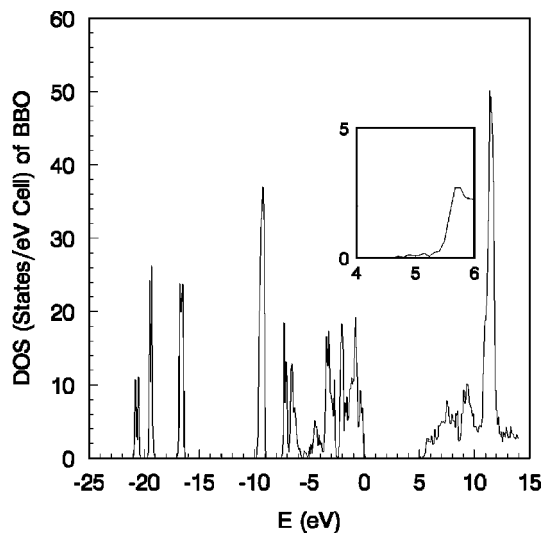


FIG. 8. Total DOS of BBO crystal.

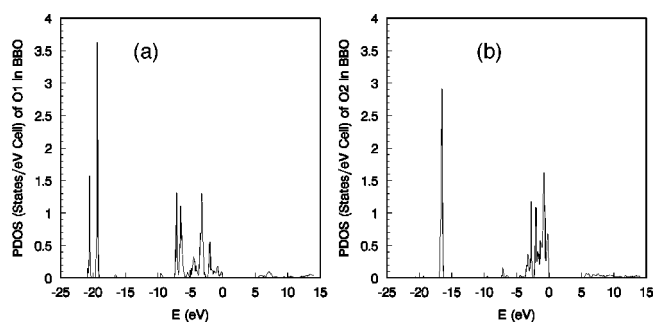


FIG. 9. Partial DOS projected on oxygen atoms of BBO. That on O3 atom is similar to O1, and that on O4 atom is similar to O2.

The $5p$ semicore states of Ba forms a local band centering at about -9 eV in the VB region (Figs. 8 and 10). This is well known in the experiments as discussed below.

The CB structures of CBO and BBO are qualitatively similar to each other, but distinct from LBO crystal, so that an obvious $6s$ cation band appears at the bottom about 1 eV below other dense bands [Figs. 2(b) and 7]. The total DOS of BBO, which are calculated at 35 special \vec{k} points, has also three peaks in the CB region (Fig. 8), which mainly originates from Ba $6s$, $5d$, and $4f$ (Fig. 10), in the energy order, respectively. The B-O bonds start from above 5.7 eV, about 1 eV above the CB bottom (Figs. 9 and 11).

C. Comparison with literatures

From Table II, the average $1s$ binding energy at O1 (or O3) in BBO crystal changes by about 2.88 eV compared to that at O2 (or O4). It is comparable to the measured difference 2.4 eV, estimated from Fig. 6 in Ref. 6. The calculated position of the Ba $5p$ peak (-9 eV) deviates slightly from the measured value [-12 eV (Ref. 6)] for the default of LDA that core-hole correlation has not been considered. Besides, the measured Ba $5p$ semicore peak is a doublet with splitting about 2.5 eV, unlike the singlet of present result (Figs. 8 and 10), which, as suggested in Ref. 8, could be attributed to the neglect of the spin-orbit splitting in the calculation.

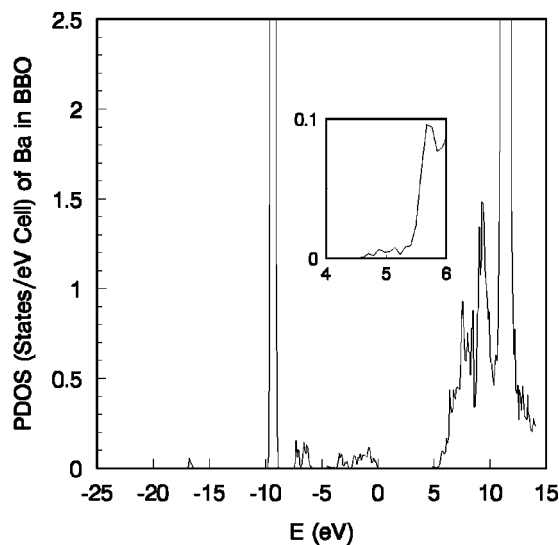


FIG. 10. Partial DOS projected on the barium atom of BBO crystal.

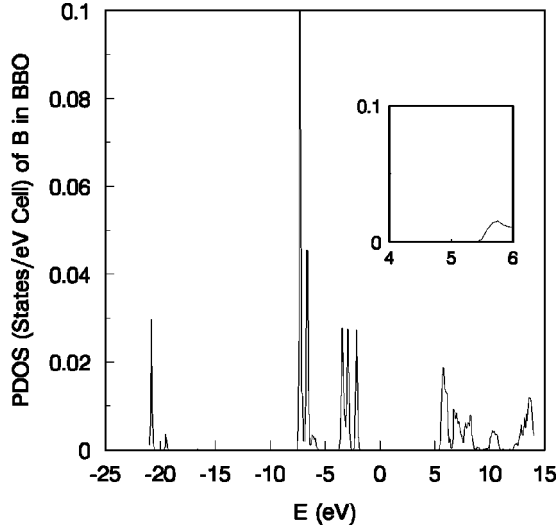


FIG. 11. Partial DOS projected on the boron atom of BBO crystal. B1 and B2 atoms have similar profiles.

According to the calculation of Xu, Ching, and French,⁸ for LBO the direct band gap is 7.37 eV at Γ ; for BBO, the indirect band gap is 5.52 eV from Γ to X , with the direct band gap 5.61 eV at Γ . It is slightly different from our results. The bottom of CB in our calculation is at Z , not at X . Hsu and Kasowski⁹ reported that the band gaps of LBO and BBO are 6.9 eV and 4.9 eV, respectively, closer to our results. However, they did not give the gap position in the Brillouin zone. The general profiles of the total DOS of LBO and BBO have no obvious difference between Xu, Ching, and French and ours. In the three different band calculations, Xu, Ching, and French,⁸ Hsu and Kasowski,⁹ and the present, the VB top of the LBO and BBO originates from the states of anionic groups. They also agree that for the CB bottom of LBO the cation gives little contribution, while for BBO the cation has a dominant contribution.

III. LINEAR OPTICAL PROPERTIES

Calculation of the linear optical properties using LAPW method has been discussed in detail in our recent work.¹⁴ Within the one-electron picture, the interband optical conductivity tensor reads (atomic units)

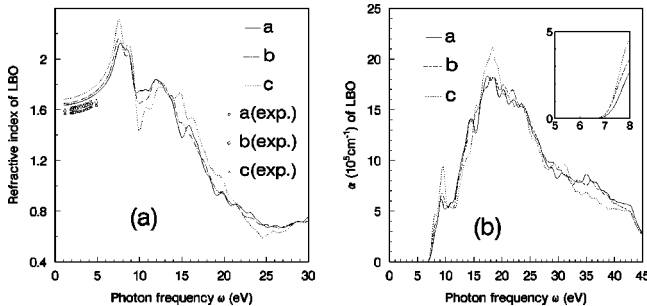


FIG. 12. Refractive index and linear absorption coefficients α of LBO crystal. The labels a , b , and c represent the polarization directions of the photon along the crystal axes a , b , and c , respectively.

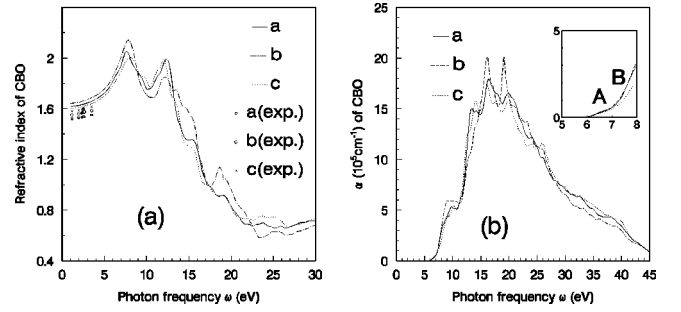


FIG. 13. Refractive index and linear absorption coefficients α of CBO crystal. The labels a , b , and c represent the polarization directions of the photon along the crystal axes a , b , and c , respectively.

$$\sigma(\omega) = \frac{2\pi}{\omega\Omega} \sum_{\vec{k}} W_{\vec{k}} \sum_{c,v} | \langle c | \vec{e} \cdot \vec{p} | v \rangle |^2 \delta(E_c - E_v - \omega), \quad (1)$$

where Ω is the cell volume, ω the photon energy, \vec{e} the polarization direction of the photon, and \vec{p} the electron momentum operator. The integral over the k space has been replaced by a summation over special \vec{k} points with corresponding weighting factors $W_{\vec{k}}$. The momentum matrix elements are evaluated at the same special \vec{k} points as used in the calculation of the DOS. The second summation includes the VB states (v) and CB states (c), and the subscript E is the corresponding band energy. In Eq. (1), it has been assumed that in these wide gap crystals the VB is fully occupied while the CB is empty.

The imaginary part of the complex dielectric function $\varepsilon_2(\omega)$ is evaluated from the optical conductivity $\sigma(\omega)$ according to $\varepsilon_2(\omega) = 2\pi\sigma(\omega)/\omega$. Then the real part of the dielectric function $\varepsilon_1(\omega)$ is obtained by the Kramers-Kronig relation. Thus the static dielectric constant in the long-wavelength limitation is given by $\varepsilon_0 = \varepsilon_1(0)$. From the complex dielectric function, the linear refractive index reads

$$n(\omega) = \left(\frac{\sqrt{\varepsilon_1^2(\omega) + \varepsilon_2^2(\omega)} + \varepsilon_1(\omega)}{2} \right)^{1/2},$$

and the linear absorption coefficient is related to ε_2 by $\alpha = \varepsilon_2\omega/(nc)$, where c is the velocity of light in the vacuum.

In Figs. 12(a), 13(a), and 14(a), the calculated refractive

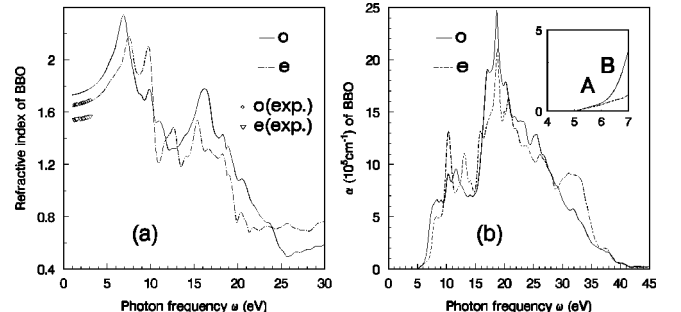


FIG. 14. Refractive index and linear absorption coefficients α of BBO crystal. The label o represents polarization perpendicular to the threefold rotation axis; and e along it.

TABLE III. Static dielectric constants (ϵ_0) and birefringent indexes Δn of LBO, CBO, and BBO crystals.

		ϵ_0 along axes			Δn
		<i>a</i> or <i>o</i>	<i>b</i> or <i>e</i>	<i>c</i>	
LBO	Present	2.66	2.71	2.82	0.048
	Expt.	2.45	2.53	2.58	0.041
	Ref. 8	2.57	2.72	2.81	
BBO	Present	2.98	2.68		0.089
	Expt.	2.74	2.38		0.113
	Ref. 8	2.82	2.70		
CBO	Present	2.60	2.68	2.55	0.040
	Expt.	2.31	2.40	2.49	0.058

indexes of LBO, CBO, and BBO crystals with different polarization directions are plotted together with available experimental data. It shows that the slight optical anisotropies are reproduced in the calculation. The anisotropic orders of LBO and BBO are in good agreement with the measurement, but that of CBO deviates from the measured one. The static dielectric constants are listed in Table III. The measured data are estimated from the refractive indexes at the measured longest wave length in the transparent region.^{3,20,21} The relative errors of the calculated values are less than 15% with respect to the measured ones. The birefringent index is also listed in Table III. The calculations of LBO and BBO are in very good agreement with the measured data and that of the previous calculation⁸ as shown in Table III, but CBO deviates in that it is larger in its magnitude from the experiment and in the wrong trend with respect to LBO.

The calculated linear absorption spectra are plotted in Figs. 12(b), 13(b), and 14(b) for LBO, CBO, and BBO crystals, respectively. Three dominant features arise from these figures as follows. (i) LBO and CBO have similar general profiles in their frequency dependence. Both LBO and CBO begin with a narrow shoulder at about 10 eV, then follows a set of strong peaks after about 12 eV. However, in BBO the shoulder extends over a wide range from about 8 to 15 eV. This might be due to its peculiar valence-band structure. (ii) The onset of the absorption of LBO [inset of Fig. 12(b)] is a sharp increase and coincides almost exactly with region *B* in the CBO absorption spectrum at about 1 eV above the gap edge [inset of Fig. 13(b)]. This indicates that LBO and CBO have the same mechanism of the optical transition at these energy positions. (iii) The absorption spectra of CBO and BBO crystals have another region *A* in the neighborhood near their gap edges, which is a slowly increasing region. This causes the band gap of CBO to be lower than that of LBO, although the overall absorption characteristics of the two crystals are the same. Considering the difference of the CB states and similarity of the VB top states between LBO and CBO and inspecting the transition processes in the low-energy regions, it is found that region *A* is due to the interatomic transition from the anionic group to the cation. In contrast, region *B* is the intraatomic transition within the anionic group. Furthermore, the large difference in the magnitude between regions *A* and *B* infers that the dominant contribution to the optical transition in these borate crystals is between the states within the anionic groups, i.e., intraatomic transitions.

Present result of linear absorption spectra of LBO [Fig. 12(b)] compares well with Xu and Ching (Fig. 3 in Ref. 7), though the shoulder at about 10 eV is more prominent there. However, the absorption spectra given by Xu, Ching, and French⁸ for BBO differs from the present result [Fig. 14(b)] and experiment (curve shown in Fig. 10 of Ref. 8) at the near gap edge region. Their spectra failed to reveal the slowly increasing absorption region (*A*).

IV. DISCUSSION AND CONCLUSION

From previous discussions on the electronic structure, it is concluded that LBO and CBO crystals have qualitatively similar VB structures resulting from the same anionic group, while on account of the similarity of cations CBO and BBO crystals have qualitatively similar CB structures. Cations have important impacts on the CB bottom as the atomic number of cations increases, as exhibited by the fact that the band gap of CBO is lowered by the cation compared to LBO. The HOMO dangling bonds of both the $(B_3O_7)^{5-}$ and $(B_3O_6)^{3-}$ groups have evolved into the top of VB in these borate crystals, but the linkage of the $(B_3O_7)^{5-}$ group lowers the energy of the dangling bonds and enlarges the band gap by about 2.2 eV. This is the main cause of the gap of LBO and CBO crystals being larger than BBO's.

In LBO, when the photon energy is larger than the band gap, the absorption coefficient increases abruptly. The involved initial states are mainly O derived states and the final states contain mainly the B-O bonds arising from trigonal boron atoms. Because there exist intra-atomic transitions, the absorption coefficient rises rapidly from the onset of the spectra. Though the heavy cations dominate the bottom of CB in CBO and BBO, they dramatically exert less affections on the optical transition than the anionic groups do. Thus, in CBO and BBO, the onset of spectra is a slowly increasing step, about 1 eV in width, where the valence electrons transit from the O derived initial states to the cation-derived final states. Because it is an interatomic transition, the absorption coefficients are not large. Only when photon energies are more than 1 eV above the band gap, and the final states contain the contribution of the B-O bonds, the absorption becomes strong. Indeed, rather complicate structure has been observed in the absorption spectra of the BBO,²² however, the experimentalists did not interpret it as induced by structures in conduction bands. The large difference between the intra- and inter-atomic transition in the magnitude should also be meaningful to the understanding to the second order NLO susceptibility, however, where the integrated effects of the whole CB's as the intermediate states are to be considered.

ACKNOWLEDGMENTS

The authors thank Dr. Xuebin Chi for the parallelizing eigen-solver and Professor Chuangtian Chen for fruitful discussion. This work was supported by the National Science Foundation of China (Grant No. 19474063). Support in computing facilities from the National Research Center of Intelligent Computing, Chinese Academy of Sciences, and from the Computer Network Information Center is gratefully acknowledged.

- ¹C. T. Chen, B. C. Wu, A. D. Jiang, and G. M. You, *Sci. Sin. Ser. B* **28**, 235 (1985).
- ²C. T. Chen, Y. C. Wu, A. D. Jiang, B. C. Wu, G. M. You, R. K. Li, and S. L. Lin, *J. Opt. Soc. Am. B* **6**, 616 (1989).
- ³Y. C. Wu, T. Sasaki, S. Takai, A. Yokotani, H. Tang, and C. T. Chen, *Appl. Phys. Lett.* **62**, 2614 (1993).
- ⁴C. T. Chen, *Sci. Sin.* **22**, 756 (1979).
- ⁵C. T. Chen, Y. C. Wu, and R. K. Li, *Phys. Lett.* **2B**, 389 (1985).
- ⁶R. H. French, J. W. Ling, F. S. Ohuchi, and C. T. Chen, *Phys. Rev. B* **44**, 8496 (1991).
- ⁷Y. N. Xu and W. Y. Ching, *Phys. Rev. B* **41**, 5471 (1990).
- ⁸Y. N. Xu, W. Y. Ching, and R. H. French, *Phys. Rev. B* **48**, 17 695 (1993).
- ⁹W. Y. Hsu and R. V. Kasowski, *J. Appl. Phys.* **73**, 4101 (1993).
- ¹⁰Wendan Cheng, Jiayi Lu, *Chin. J. Struct. Chem.* **16**, 81 (1997).
- ¹¹V. H. König and R. Hoppe, *Z. Anorg. Allg. Chem.* **439**, 71 (1978).
- ¹²J. Krogh-Moe, *Acta Crystallogr., Sect. B: Struct. Crystallogr. Cryst. Chem.* **30**, 1178 (1974).
- ¹³R. Fröhlich, *Z. Kristallogr.* **168**, 109 (1984).
- ¹⁴J. Li, C. G. Duan, Z. Q. Gu, and D. S. Wang, *Phys. Rev. B* **57**, 2222 (1998).
- ¹⁵H. Krakauer, M. Posternak, and A. J. Freeman, *Phys. Rev. B* **19**, 1706 (1979).
- ¹⁶D. D. Koelling and B. N. Harmon, *J. Phys. C* **10**, 3107 (1977).
- ¹⁷J. C. Sun, J. X. Deng, J. W. Cao, D. S. Wang, W. Q. Zhang, and J. Li, *Chin. Sci. Bull.* **42**, 818 (1997).
- ¹⁸Xuebin Chi, Jun Li, and D. S. Wang (unpublished).
- ¹⁹L. Pauling, *The Nature of The Chemical Bond* (Cornell University Press, Ithaca, NY, 1960), Chap. 13, p. 504.
- ²⁰S. Lin, Z. Sun, B. Wu, and C. Chen, *J. Appl. Phys.* **67**, 634 (1990).
- ²¹V. G. Dmitriev, G. G. Gurzadyan, and D. N. Nikogosyan, *Handbook of Nonlinear Optical Crystals* (Springer-Verlag, Berlin, 1991), p. 78.
- ²²G. Zhang, Y. Yang, and C. Zhang, *Appl. Phys. Lett.* **53**, 1019 (1988).